Discussion on Biomedical Image Acquisition and Processing

Chen-I Lin, Fu-Shin Lee, Hsiao-Chi Ling, Antony Chiang and Pin-Hsien Ho

Discussion on Biomedical Image Acquisition and Processing

Chen-I Lin

College of Mechanical and Electrical Engineering Wuyi University Wuyishan 354300, China cooper0688@gmail.com

Fu-Shin Lee

Mechatronical Engineering Institute Huafan University Taipei 22301, Taiwan fslee@huafan.hfu.edu.tw

Hsiao-Chi Ling

Department of Marketing Kainan University Taoyuan 338, Taiwan max.ling911@msa.hinet.net

Antony Chiang

EDA Medical Device Technology Inc. Taichung 407, Taiwan tachiang@ms1.hinet.net

PIN-HSIEN HO

Mechatronical Engineering Institute Huafan University Taipei 22301, Taiwan acb216652@gmail.com

ABSTRACT - The purpose of this article is to design an optical scanning probe mechanism for capturing biomedical tissue images through an USB camera and to develop an FPGA embedded image processing firmware for image cropping, rotation, sharpening, and stitching, especially, as to synchronize with the scanning probe mechanism. The FPGA embedded firmware then successively displays each built image after stitching several scanned images on an LCD screen. Meanwhile, the research applied the 3D printing technology to prototype the probe mechanism assembly using a SolidWorks model for the probe mechanism and associated fixtures as well as servomotors. The optical fiber probe mechanism successfully accomplished the scanning motions as capturing images within extended regions. The research develops the FPGA embedded firmware on a Linux OS platform and installs the codes on a DE10-Nano Kit FPGA development board. Verification through the prototype optical probe mechanism to scan the extended area and collect multiple tissue images to construct a widened image after switching effectively.

KEYWORDS - optical fiber scan, image stitching, image processing, and FPGA.

I. INTRODUCTION

With advancements of science and technology, human livings in all aspects become more comfortable, but science developments with associated technologies also bring harmful side effects to the environments, especially generated pollutions harm human health seriously. Hence, biomedical technology developments become more important during last two decades. biomedical technology has proposed minimal invasive surgery techniques through endoscopy or other imaging techniques, allowing doctors to complete surgery without generating large scale wounds, which imply that surgeons are able to observe internal tissues inside a human body through endoscopy with small wounds. Therefore, this research aims to develop an optical scanning probe endoscopy for acquiring and processing biomedical tissue images. The paper designed and coded acquiring/processing firmware for the scanning probe first and then performed data collections through scanning optic fiber manipulations. The system controls the moving image fiber carrier through embedding developed codes into an FPGA circuit board, and hence generates inspected target images using the scaning prototype system. Captured multiple biomedical tissue images after scanning then integrate into extened tissue through image stitching techniques. Through the developed endoscope prototype using the scanning fiber needle module, it is feasible to inspect tens of times of image area as compared with the original fiber observation range.

II. METHOD

A. *Program design of optical fiber scanning mechanism and imaging office*

2.1 *Design of optical fiber scanning mechanism*

Note that it is impractical to use rigid needle fibers in the systems, the research employs a flexible optical fiber needle and an USB camera, with the fiber needle directly attached to the USB camera lens. The prototyped mechanism drives the optical fiber carrier to move in two directions, allowing the imaging needle to scan the observation tissue plane and capture the inspected biomedical images. The research utilized the SolidWorks tool to design the optical fiber scanning mechanism and fabricate the device through a 3D printer. Within the mechanism, two servo motors convert their rotational power into linear movements through two gear-and-rack sets. With the 3D printer fabrication capacity, size limit, and designated movement accuracy, it is straightforward to apply a gear-and-rack movement formula as follows:

$$l = \frac{z\theta}{360°}\pi m \tag{2-1}$$

Where θ is the rotation angle of the gear, l is the displacement of the rack, z is the number of gear teeth, and m is the modulus of the gear. The relationship between the number of teeth m and the pitch circle diameter d:

$$m = \frac{d}{z} \tag{2-2}$$

The above two formulas design the gear to rotate every 1 °, which drives the rack to move 0.2 mm. According to the actual 3D printer accuracy, set the formula (2-1) and formula (2-2) gear and rack combination parameters as follows:

Gear:	Rack:
Modulus (m): 1	Modulus (m): 1
Pressure angle (α): 20 °	Pressure angle (α): 20 °
Number of teeth (z): 28	
Pitch circle diameter (d): 28 mm	

SolidWorks designs and draws the gear and rack combination according to the parameters of the gear and rack. Figure 2-1 shows the assembly drawing of the matching mechanism. The mechanism drives the image needle carrier to perform vertical and horizontal plane scanning operations, and then add a USB camera and fiber optic image needle. Figure 2-2 shows the combination.
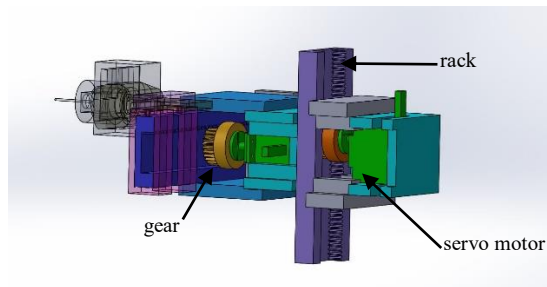

Figure 2-1 Optical fiber scanning horizontal and vertical displacement mechanism
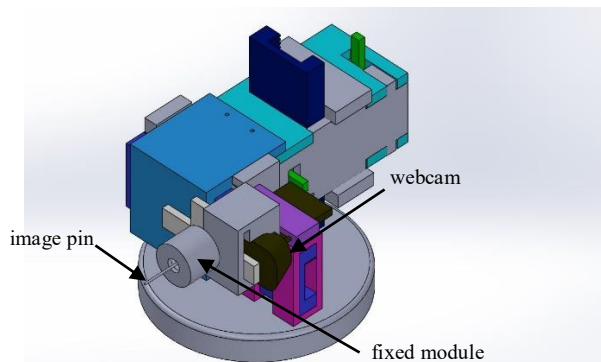

Figure 2-2 Optical fiber scanning mechanism combination in SolidWorks

2.2 Programming of the imaging office

The USB camera captures an image with a fixed fiber image on the carrier. Keep the required parts and cut without the image. Then, because the fiber only fixes the image pin at one end, there is an angle deviation of about 20 ° between the input image and the output image. After cutting, you need to rotate the image processing to restore the original angle, as shown in Figure 2-4.

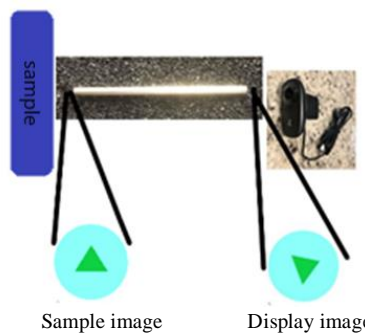Sample image   Display image
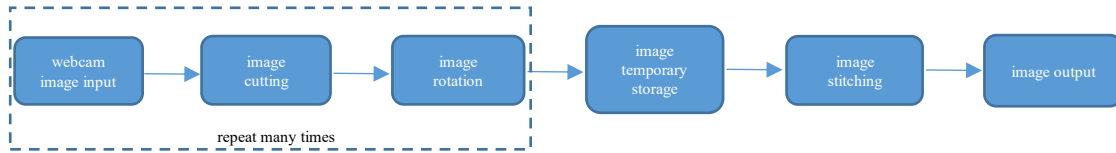
Figure 2-3 Schematic diagram of image pin rotation

Figure 2-4 Image processing flow

After the above process, restore the original state image and divide the storage space into temporary storage programs. After capturing multiple images and storing them in the memory space, stitch the images according to the program settings, and then output the images to the display screen after completion, which is the entire process of the fiber-scanning image stitching process. The following paragraphs briefly describe the processing methods of each segment of the image-needle acquisition data.

- *Image cutting*

The USB camera captures images of biomedical tissues including the target and the surrounding area. First, cut off the non-target image area. A target range can be set in the image area and then images within or can choose outside the range.

Can choose outside the range. The image drawing coordinates are in pixels, the upper left corner is the origin of (0,0), and the right and down are positive. Access to the image in the selected calibration area, as shown in Figure 2-5, a selected area is marked at image A ((In red frame), save image A as image B by executing the source code, and access the image in the selected calibration area.
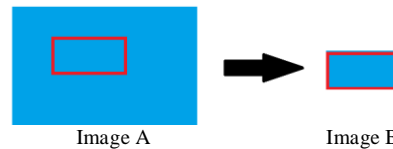

Image A   Image B
Figure 2-5 Schematic diagram of image cutting

- *Image translation, rotation, zoom*

Convert the original pixel coordinates of the image to new coordinates and perform the geometric transformation of image rotation through spatial transformation and gray level interpolation. The development uses nearest-neighbor interpolation.

Use the following formula to calculate the image coordinate space transformation:

$$\begin{bmatrix} x' \\ y' \end{bmatrix} = \begin{bmatrix} a & b \\ c & d \end{bmatrix} \begin{bmatrix} x \\ y \end{bmatrix} + \begin{bmatrix} e \\ f \end{bmatrix} \tag{2-3}$$

Where (x, y) is the original pixel coordinates, (x ', y') is the converted coordinate, e and f are the translation amount of the image in the x and y directions respectively, formula (2-3) includes translation, scaling and rotation Calculation, integration is expressed by transformation matrix M. For example, the scale transformation matrix M_{pan} is:

$$\mathbf{M}_{pan} = \begin{bmatrix} 1 & 0 & e \\ 0 & 1 & f \end{bmatrix} \tag{2-4}$$

Enlarge a1 time's image in the x-direction and b1 times in the y-direction. The transformation matrix M_{scale} is:

$$\mathbf{M}_{scale} = \begin{bmatrix} a_1 & 0 & 0 \\ 0 & b_1 & 0 \end{bmatrix} \tag{2-5}$$

The image rotation rotates counter clockwise θ degrees around the origin, and the transformation matrix M_{rot} is:

$$\mathbf{M}_{rot} = \begin{bmatrix} \cos\theta & \sin\theta & 0 \\ -\sin\theta & \cos\theta & 0 \end{bmatrix} \tag{2-6}$$

Example Figure 2-6 (a) After the image is rotated and calculated by the formula (2-6), the image of Figure 2-6 (b) can be obtained.

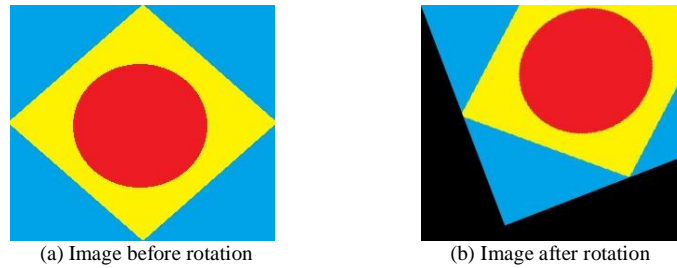| (a) Image before rotation | (b) Image after rotation |

Figure 2-6 Image rotation processing

- *Image stitching*

Image stitching combines two or more (including partially overlapping) images into one image, and the calculation process is divided into image matching, image synthesis, and setting camera parameters. The same target is shot by different cameras or different exposure values, and there is a slight gap in obtaining individual images. Therefore, when processing multiple images, different cameras or exposure value sources need to be considered, and the camera parameters must be averaged and adjusted consistently. Here, a fixed camera and exposure are used. Value decreases impact.

Image matching includes two parts: feature point calculation and matching. Among them, feature point search and description methods, such as SIFT and SURF are protected by PATENT. The ORB calculation method is used in the experiment.

The ORB feature point calculation method is used to find the feature points in the image with FAST (features from accelerated segment test), mainly to find the special convex points in the image. Set the pixel to be detected as P. As shown in Figure 2-7, draw a circle with 3 pixels and a radius of P as the center of the circle. Of the 16 pixels (N1 ~ N16) on the circle, if there are t consecutive pixels and When the gray value of point P is different, P is the feature point, where t is the feature point, and the threshold is generally set to 12 during detection.
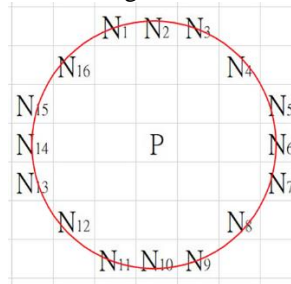

Figure 2-7 Schematic diagram of FAST algorithm

The definition of ORB feature points uses the BRIEF descriptor. The feature point P is the center of the circle, and d is the radius. Draw a circle as shown in Figure 2-8. The circle contains N pairs of feature points. Generally, N takes 512 or 256. The example uses N = 5 Feature point pair description.
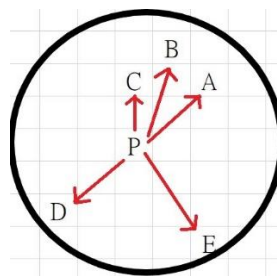

Figure 2-8 BRIEF descriptor description

The mark pairs in Figure 2-8 are P1 (P, A), P2 (P, B), P3 (P, C), P4 (P, D), and P5 (P, E). The five-point pair defines its binary value with the formula T.

$$T\big(P_N(A,B)\big) = \begin{cases} 1, & A > B \\ 0, & A \leq B \end{cases} \tag{2-7}$$

That is, formula (2-7) compares the gray value of the two feature point pixels of A and B, and gives the binary value described as the comparison result. Set P1 ~ P5 as compared with the above formula (2-7) to obtain:

$$T(P_1(P, A))=0$$

$$T(P_2(P, B))=1$$

$$T(P_3(P, C))=0$$
$$T(P_4(P, D))=1$$
$$T(P_5(P, E))=1 \tag{2-8}$$

Then the descriptor of the characteristic point P is 01011. The calculation is repeated for each feature point to obtain the feature point description of the image, and then the matching is completed by comparing the feature point descriptors. The process compares the value of the co-located position of the descriptors of the two image feature points. If more than 80% of the positions are the same, it is regarded as the same feature. For example, in Figure 2-9, the red feature point descriptor of image A is 01011, the yellow feature point descriptor is 11111, and the green feature point descriptor is 00000, the red feature point descriptor of image B is also 01010, and the yellow feature point descriptor is 11110, and the purple feature point descriptor is 10100. Comparing the six feature point descriptors, since the red feature point descriptors of image A and image B are all 01011, it is determined that the two feature points in the two images should be the same point. The yellow feature point descriptor of image A is 11111, and the image B is 11110, 80% of the two are the same, so the yellow feature points of image A and image B are determined to be the same point. The difference between the green feature point of image A and the purple feature point of image B is greater than 80%, so it is judged that the two are different points, and the feature points in the two images are matched according to the cycle comparison.
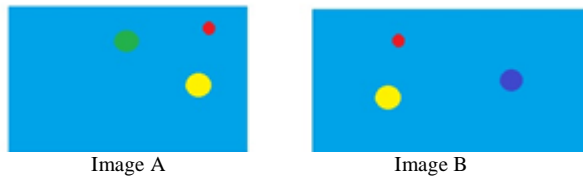

| Image A | Image B |

Figure 2-9 Schematic diagram of feature point matching

After the two images are matched, the two images are synthesized according to the feature points and the results, and the two steps of finding and fusing for the seam are respectively performed. First, calculate the position of the seam line in the image overlapping area, and the two ends of the seam line belong to different image sources. Only through the seam line synthesis produces obvious borders in the overlapping area, and it is necessary to eliminate the obvious borders of the overlapping area through fusion processing to complete the smooth fusion of the image.

The above-mentioned image stitching process is searched by the point-by-point method, and the overlapped part is mainly used to calculate the positioning seam line according to the pixel value of the corresponding position of the image according to the closer pixel image. The image boundary fusion processing adopts feathering, smoothing and blurring the areas on both sides of the seam line, and softening and naturalizing the area image at the seam line.

III. VERIFICATION EXPERIMENT

3.1 Scanning fiber optic image module test

First, the USB camera test is used to capture the image by scanning the fiber optic image pin, that is, the image pin scans RGB three-color paper as shown in the sample in Figure 3-1, and the individual image probe fiber captured image in Figure 3-2 is obtained.

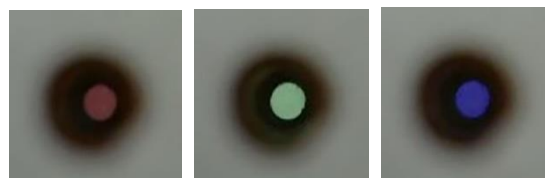Figure 3-1 RGB three-color drawing sample

Figure 3-2 The image pin captures the three-color drawing image

General image resolution refers to the CCD resolution or screen display resolution. The difference between the two definitions is to describe the objects differently. The experiment directly tests the resolution of the lens to the image. The image needle diameter is only 800 μm and the resolution test sample diagram shown in Figure 3-3 is used to complete the system lens to image resolution test.
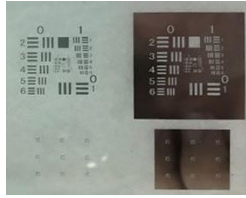
Figure 3-3 1951 USAF resolution test sample diagram

Using the 1951 USAF resolution test chart, the resolution can be calculated as follows:

$$R(\frac{lp}{mm}) = 2^{G + \frac{E-1}{6}}$$

(3-1)

Where R is the optical resolution (resolving power of the optical imaging system), the unit is line pairs per millimeter, G is the Group Number, which is the red box in Figure 3-4, and E is the element (Element), which is Figure 3- 4 in the blue circle. According to the formula, each picture represents the optical resolution. The 1951 USAF resolution test chart should be directly compared to Table 3-1. The resolution range is 1 lp / mm to 228 lp / mm, where lp / mm is the number of line pairs per millimeter. As shown in Figure 3-4, the yellow circle is the first unit of group 0, corresponding to a resolution of 1 lp / mm, that is, a 0.5 mm wide line and a 0.5 mm wide space can be distinguished within 1 mm.
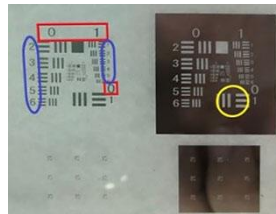

Figure 3-4 Schematic diagram of group number (red frame) and unit (blue frame)

TABLE 3-1 1951 USAF resolution test chart corresponding to optical resolution (lp / mm)

Unit \ Number	0	1	2	3	4	5	6	7
1	1.00	2.00	4.00	8.00	16.00	32.0	64.0	128.0
2	1.12	2.24	4.49	8.98	17.95	36.0	71.8	144.0
3	1.26	2.52	5.04	10.10	20.16	40.3	80.6	161.0
4	1.41	2.83	5.66	11.30	22.62	45.3	90.5	181.0
5	1.59	3.17	6.35	12.70	25.39	50.8	102.0	203.0
6	1.78	3.56	7.13	14.30	28.50	57.0	114.0	228.0

In the experiment, the 3rd group of the 1951 USAF resolution test chart was used to perform the image pin scan test.

Figure 3-5 (a) (b) (c) (d) shows the captured images respectively. Group 6 unit pairs, but the image of each unit in the fourth group cannot be clearly displayed at the beginning. Judging from the optical image needle composed of 0.009 mm diameter fiber, the resolution limit is about 14.30 lp / mm, and 0.0345 mm can be distinguished size.
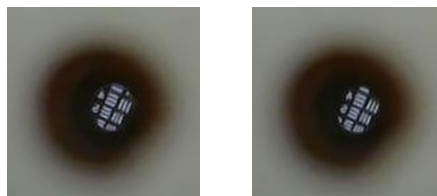
(a) Group 3, Unit 4   (b) Group 3, Unit 5
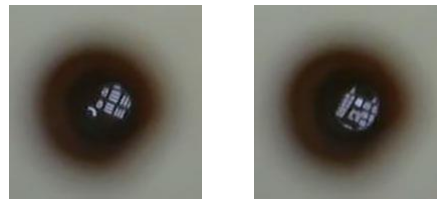
(c) Group 3 Unit 6   (d) Group 4 Unit 1

Figure 3-5 1951 USAF resolution test chart clarity identification experiment

3.2 Scanning fiber image processing program verification

- *Image cutting and rotation*

In the image needle scanning experiment, it is necessary to pay attention to the USB camera to capture the image target area and then perform the image stitching and stitching process. Experimental process Crop rotation processing Figure 3-6 shows the original probe to capture images to obtain images after cropping as shown in Figure 3-7 (a), and images after rotation as shown in Figure 3-7 (b).
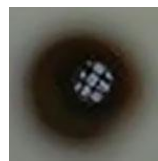

Figure 3-6 The original captured image of the probe

(a) Crop the processed image   (b) Rotate the processed image

Figure 3-7 Results of cropping and rotating image processing

- *Image clarity*

The image pin scanning process may cause image blur due to the movement of the vehicle. The image obtained during the capture process needs to be sharpened. Although it can strengthen the blurred image but also highlight the image noise, the experiments are compared separately: (i) The original image is only sharpened; (Ii) The original image is blurred to remove noise and then sharpened. Table 3-2 shows the results.

Table 3-2 Image clarity test

Original image	Sharpen only	Sharpen after blurring

Table 3-2 shows that only sharpening the enhanced image will simultaneously enhance the noise, but blurring and then sharpening can be avoided. The human eye cannot tell whether there are obvious differences in sharpening processing, but sharpening strengthens the image features and helps to improve the subsequent image stitching processing effect.

In the image stitching experiment test, the original image sample of a 1951 USAF resolution test chart as shown in Figure 3-3 is cut into 9 images covering overlapping regions, as shown in Figure 3-8. In the experiment, input part and set four sets of partial images with different boundaries after cutting, rotating and stitching of the original code of the embedded board. The first set of 01 ~ 09 partial images, the second set of 01 ~ 08 partial images, the third set of 01 ~ 06 partial images, and the fourth set of 01 ~ 04 and 06 ~ 09 part of the image. Table 3-3 and Table 3-4 show the image output obtained by grouping.
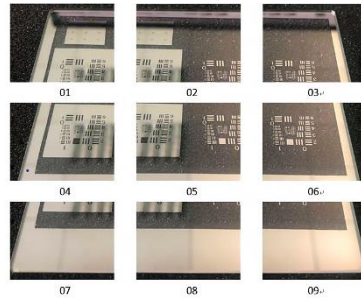
Figure 3-8 Cutting images covering each part of the overlapping area

Table 3-3 Image stitching test group (top)

Number of groups	First group	Second Group
Input image	01~09	01~08
Set boundaries		
Image stitching output map		

Table 3-4 Image stitching test group (below)

Number of groups	The third group	Fourth group
Input image	01~06	01~04、06~09
Set boundaries		
Image stitching output map		

Table 3-3 and Table 3-4 are groups. The first group of experiments (input images from 01 to 09) and the output image has the same complete rectangle as the original image, and the synthesis result is the same as the original image without any distortion. Then enter eight images from 01 to 08 in the experiment, set a rectangular gap in the lower right corner of the image boundary. The synthesis result is the same as the first group of results, and display a black gap at the original number 09 image position, and the output matches the original setting without distortion. The third set of experiments (input 01 ~ 06 images) set the image below the boundary there is a difference between the upper and lower non-horizontal, the output synthesis results are not distorted, and the black is displayed at the gap to match the original setting. From 06 to 09 eight images, and there is a missing block in the canter of the set of images. The output synthesis result has no distortion, and the black area in the canter shows that the black is consistent with the original setting. Four sets of experiments show that the developed system satisfies the matching feature point identification, and has high stitching to restore images in the same plane, and can use image probe scanning to capture a wide range of biomedical tissue images.

- *Electromechanical integration of image module and mechanism*

The image needle scanning suture test scans the third group 1 to 6 units of the 1951 USAF resolution test chart by controlling the optical fiber-probe carrier. The test process controls the motor rotation of Figure 2-2 to scan, and captures an image every 1 degree of rotation. Scanning resolution test chart The third group 1 to 6 units are shown in Figure 3-9 image (blue area), then rotate to cut The results of the captured images are shown in Figure 3-10, each image pixel is 36 x 36.
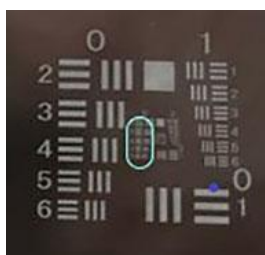
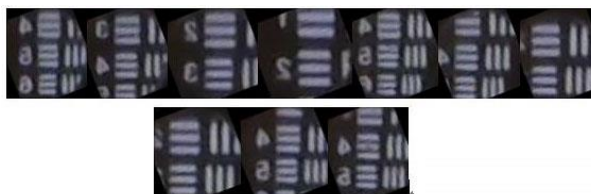Figure 3-9 Scanning area (blue circle range)

Figure 3-10 Results of fiber image scanning

Figure 3-10 captures the blue area to obtain each part of the image. After the image is directly stitched, the output is shown in Figure 3-11.

Figure 3-11 Direct image stitching results

Figure 3-10 is capture the blue area to obtain each part of the image. After blurring and sharpening, Figure 3-12 show the image stitching output, which is better than the direct image stitching result, and verify the development of the image-needle scan capture. Taking a large-scale biomedical organization process and implementing image blurring and sharpening of various parts of the image. It has the benefit of improving the stitching process of large-scale captured images.

Figure 3-12 Image stitching results after blurring and sharpening

IV. CONCLUSION AND DISCUSSION

In the research process, the three primary colors were scanned and tested to verify the feasibility of the image module to correctly identify the color. Through the resolution test, we learned the maximum resolution of the image module used in this study can reach 14.30 lp / mm, the observation range diameter is 35 μm, and observe cells with a diameter of 10μm ~ 100μm in general organisms.

The carrier module USB camera captures the image during the scanning process, which reduces the noise of scanning movement through cropping, rotation, blurring, and sharpening, and improves the recognition of adjacent image feature points. In the subsequent image stitching process, it can improve the synthesis of multiple partial images and smoothing benefit. The original image of the resolution test chart is cut after the original image is stitched, and the development system is verified to be suitable for the imaging pin of the carrier system, and the 35μm diameter observation range is 14.30 lp / mm resolution. After scanning and capturing multiple images suture, obtain a large range of biomedical tissue observation images, complete the prototype mechanism of the optical fiber probe scanning suture image.

ACKNOWLEDGMENT

REFERENCES

1. D. Callen and M. Schulze, 2014, "Laser combiner enables scanning fluorescence endoscopy," *BioPhotonics*, November 28.

2. Brown, M. and Lowe, D. (2003), "Recognizing panoramas," ICCV '03 *Proceedings of the Ninth IEEE International Conference on Computer Vision*, Volume 2, Page 1218, Nice, France.

3. Lowe, David G., "Object recognition from local scale-invariant features," *Proceedings of the International Conference on Computer Vision*: 1150–1157. 1999.

4. 黄汉哲，2009，SIFT 算法应用于航测影像拼接之研究，国立中山大学，海洋环境及工程学系。

5. 曹博舜，2018，*以保距空拍影像拼接提供地面对象定位*，国立交通大学，网络工程研究所。

6. 许迪翔，2017，*用于行车侧方环景影像拼接安全系统*，国立台北科技大学，电子工程系。

7. 风吴痕，2017，OpenCV *实践之路—圆形切割和矩形切割*，检自 https://blog.csdn.net/wc781708249/article/details/78588570(June .25 2019)。

8. xiaowei_cqu，2012，【OpenCV】*图像几何变换：旋转，缩放，斜切*，检自 https://blog.csdn.net/xiaowei_cqu/article/details/7616044 (June .25 2019)。

9. Ethan Rublee,Vincent Rabaud, Kurt Konolige , and Gary Bradski, 2011, ORB: an efficient alternative to SIFT or SURF, Published in: 2011 *International Conference on Computer Vision*.

10. 吴仁豪，2015，*手术用具精密微动平台自动化系统研制*，华梵大学，机电工程学系

11. 陈智宇，2017，CANopen *技术之并联机构应用*，华梵大学，机电工程学系。

12. Jaeyoung Yoon and Daeho Lee, 2017, "Real-Time Video Stitching Using Camera Path Estimation and Homography Refinement," *Symmetry*, Volume 10, Issue 1 (January 2018).

13. 陈伟麟，2011，*扫描式光纤内视显微术应用于非线性光学影像*，国立成功大学，光电科学与工程研究所。